Haloalkane Dehalogenases: Steady-State Kinetics and Halide Inhibition†

John F. Schindler,‡ Penelope A. Naranjo,‡ David A. Honaberger,‡ Chia-Hwa Chang,§ James R. Brainard,‡ Laura A. Vanderberg,*,‡ and Clifford J. Unkefer*,‡

Chemical Sciences and Technology Division, Bioscience and Biotechnology Group, and Life Sciences Division, Los Alamos National Laboratory, Los Alamos, New Mexico 87545

Received December 3, 1998; Revised Manuscript Received March 3, 1999

ABSTRACT: The substrate specificities and product inhibition patterns of haloalkane dehalogenases from *Xanthobacter autotrophicus* GJ10 (*Xa*DHL) and *Rhodococcus rhodochrous* (*Rr*DHL) have been compared using a pH-indicator dye assay. In contrast to *Xa*DHL, *Rr*DHL is efficient toward secondary alkyl halides. Using steady-state kinetics, we have shown that halides are uncompetitive inhibitors of *Xa*DHL with 1,2-dichloroethane as the varied substrate at pH 8.2 (Cl^-, $K_{ii} = 19 \pm 0.91$; Br^-, $K_{ii} = 2.5 \pm 0.19$ mM; I^-, $K_{ii} = 4.1 \pm 0.43$ mM). Because they are uncompetitive with the substrate, halide ions do not bind to the free form of the enzyme; therefore, halide ions cannot be the last product released from the enzyme. The K_{ii} for chloride was pH dependent and decreased more than 20-fold from 61 mM at pH 8.9 to 2.9 mM at pH 6.5. The pH dependence of $1/K_{ii}$ showed simple titration behavior that fit to a pK_a of approximately 7.5. The k_{cat} was maximal at pH 8.2 and decreased at lower pH. A titration of k_{cat} versus pH also fits to a pK_a of approximately 7.5. Taken together, these data suggest that chloride binding and k_{cat} are affected by the same ionizable group, likely the imidazole of a histidyl residue. In contrast, halides do not inhibit *Rr*DHL. The *Rhodococcus* enzyme does not contain a tryptophan corresponding to W175 of *Xa*DHL, which has been implicated in halide ion binding. The site-directed mutants W175F and W175Y of *Xa*DHL were prepared and tested for halide ion inhibition. Halides do not inhibit either W175F or W175Y *Xa*DHL.

The haloalkane dehalogenases from *Xanthobacter autotrophicus* GJ10 (*Xa*DHL[1]) and *Rhodococcus rhodochrous* (*Rr*DHL) catalyze the irreversible hydrolysis of a variety of haloalkanes to the corresponding alcohol, halide, and a hydrogen ion (*1*−*3*). Interest in these enzymes stems from their potential use in remediation of environmental contaminants (*4*−*6*). Due to the elegant studies of Janssen and coworkers, many of the details of the catalytic mechanism and structure of the *Xa*DHL are understood (*7*−*12*). The active site of *Xa*DHL contains three catalytic residues, D260, H289, and D124 (*7, 8*). X-ray crystal structures (*7, 8*), site-directed mutations (*9, 10*), and mechanistic and kinetic studies (*11, 12*) on the *Xa*DHL have shown that dehalogenation of substrate occurs in four steps (Scheme 1). After formation of the Michaelis complex (Figure 1A), the side chain carboxylate of D124 acts as a nucleophile, displacing a chloride ion from the substrate and forming a covalent ester intermediate (Figure 1B). Based on the geometry of the active site and on the enzyme's absolute specificity for primary alkyl halides, the halide displacement is thought to proceed via an S_N2 type *planar* transition state (*8, 13, 14*). The next step in the pathway involves hydrolysis of the intermediate ester by hydroxide. Hydroxide is produced at the active site from a water molecule hydrogen-bonded to N_ϵ of H289. In turn, H289 is hydrogen bonded to D260. H289 accepts a water proton, and the hydroxide ion attacks the C_γ of D124 (Figure 1B,C). The product alcohol is thought to leave the enzyme as soon as it is formed. Based on pre-steady-state kinetic studies, halide ion is proposed to be the last product released from the enzyme (*11, 12*). Moreover, the release of halide from the *Xa*DHL active site is thought to proceed via a complex pathway that involves protein structural rearrangements and is proposed to be the overall rate-limiting step in the mechanism (*11*).

Scheme 1

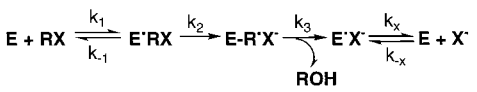

Crystal structures in the presence of chloride or iodide and under acidic conditions (pH 5.2) indicate that halide ion binds to the enzyme by interactions with two indole side chains of W125 and W175. The bound halide is located at equal distance from the N_η of W125 (3.4 Å) and N_η of W175 (3.3 Å) (*8*). A structure obtained at low pH (pH 5.2), at low temperature (4 °C), and in the presence of 1,2-dichloroethane shows substrate bound to *Xa*DHL in the trans configuration and with the leaving halide positioned between the indole NH's of W125 and W175 (3.6−3.2 Å). At pH 5.2, *Xa*DHL is not active presumably because the side chain of H289 is present as the imidizolium ion; therefore, this structure of substrate bound to *Xa*DHL at low pH (*8*) is not likely an accurate representation of the ES complex. Recently, ab

† This research was performed under the auspices of the Laboratory Directed Research and Development Program at Los Alamos National Laboratory. Los Alamos National Laboratory is operated by the University of California for the U.S. Department of Energy under Contract W-7405-ENG-36.

* Corresponding authors. E-mail: lvanderberg@lanl.gov and cju@lanl.go.

‡ Chemical Sciences and Technology Division.

§ Life Sciences Division.

[1] Abbreviations: *Xa*DHL, haloalkane dehalogenase from *Xanthobacter autotrophicus* GJ10; *Rr*DHL, haloalkane dehalogenase from *Rhodococcus rhodochrous.*

10.1021/bi982853y CCC: $18.00
Published on Web 04/14/1999

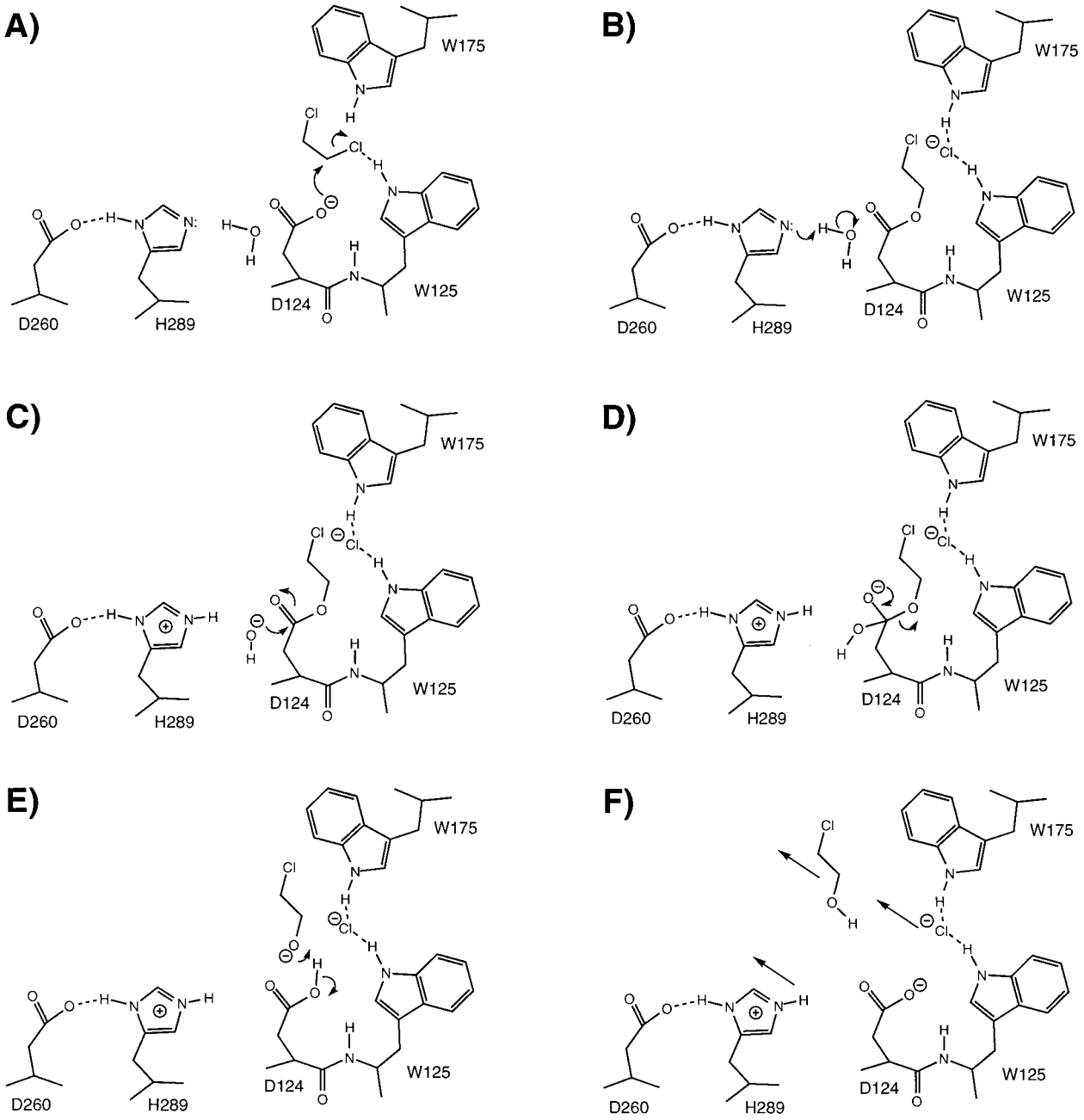

FIGURE 1: Proposed chemical mechanism of the haloalkane dehalogenase from *Xanthobacter autotrophicus* GJ10. Substrate binds to form the **E·S** complex (**A**). Nucleophilic attack by Asp124 to form an ester intermediate (**B**). A bound water is activated by His289 (**C**) for hydrolysis of the ester intermediate (**D, E**). The products alcohol, chloride, and a hydrogen ion must then leave the active site (**F**).

initio, semiempirical molecular orbital calculations, and molecular dynamics simulations were used to examine the structure of the ES complex and the S_N2 transition state (*14*−*16*). Ab initio calculations show that in the hydrophobic active site, the substrate is bound in the gauche conformation and further that the gauche conformation is required for the nucleophilic attack by the A124 carboxylate (*14*). Molecular dynamics simulations were carried out with the H289 side chain present as imidazole in the HN_δ tautomeric form with the N_δ proton hydrogen-bonded to D260. These simulations show that in the ES complex, the gauche conformation of the substrate is bound with the leaving chlorine substituent hydrogen bonded only to the indole HN_η of W125 and not to that of W175. However, in the transition state, the indole N_η protons of both the W125 and W175 are hydrogen-bonded to the leaving chlorine. In addition, site-directed mutants demonstrate that both W175 and W125 promote *Xa*DHL catalysis (*17*). Because mechanistic studies suggest that both tryptophan residues facilitate catalysis in *Xa*DHL, we expected they would be conserved throughout the family of haloalkane dehalogenases. However, alignment of the sequences of *Rr*DHL and *Xa*DHL indicates that *Rr*DHL (*2*) does not contain a tryptophan residue corresponding to W175 in *Xa*DHL (*18*) (Figure 2). Because of their differences in active site structure, we compared the substrate specificities and halide affinities of the *Rr*DHL and *Xa*DHL enzymes.

To date, dehalogenase activity has been assayed either by determining the rate of halide ion formation colorimetrically (*19*) or by determining the rate of alcohol formation by gas chromatography (*1*). Because the catalysis by the dehalogenases produces hydrogen ions as well as halide ions and alcohol, we developed an assay that monitors the steady-

```
      120       130       140       150       160       170       180
       |   **    |         |         |         |         |    *    |
XaDHL LVVQDWGGFLGLTLPMADPSRFKRLIIMNACLMTDPVTQPAFSAFVTQPADGFTAWKYDLVTPSDL
      LV+ DWG  LG      +P R K +  M       P+  P +  +     + F A++   V   +L
RrDHL LVIHDWGSALGFHWAKRNPERVKGIACME---FIRPI--PTWDEWPEFARETFQAFRTADV-GREL
```

FIGURE 2: Partial BLAST sequence alignment of *Xa*DHL (*18*) and *Rr*DHL (*2*) with active site residues marked (*). The *Rr*DHL does not contain a tryptophan corresponding to W175 in *Xa*DHL.

state kinetics by recording the absorbance change of a pH-indicator dye. This assay was convenient, even in the presence of high halide concentrations, and allowed us to determine that halides act as uncompetitive inhibitors of *Xa*DHL, but do not inhibit the *Rr*DHL enzyme. Site-directed mutants of *Xa*DHL, W175Y and W175F were no longer inhibited by halides.

MATERIALS AND METHODS

Materials. Halogenated substrates were obtained from Aldrich Chemical Co. Restriction enzymes (Novagen), expression vectors (Novagen), and Vent polymerase (New England Biolabs, Inc.) were obtained commercially. Synthetic oligonucleotides, 5′-TTACCGCC**TAT**AAATACGA-3′ (W175Y) (Biosynthesis Inc.) and 5′-TTTACCGCC**TTC**-AAATACGAT-3′ (W175F) (Oligos Inc.), were purchased. Dideoxy-termination cycle-sequencing kits from ABI Perkin-Elmer were used for DNA sequencing.

Bacterial Strains. E. coli BL21(DE3) was obtained from Novagen. *Xanthobacter autotrophicus* GJ10 (ATCC 43050) was obtained from the American Type Culture Collection (Rockville, MD). *Rhodococcus rhodochrous* NCIMB 13064 was obtained from the National Collection of Industrial and Marine Bacteria Ltd. (Aberdeen, U.K.).

Preparation of the Wild-Type and Mutant Proteins. DNA encoding wild-type GJ10 dehalogenase (*Xa*DHL) from plasmid pGemT-*DHLA* (B. Willardson, unpublished results) was amplified using the polymerase chain reaction (*20*). The primers introduced *Nde*I and *Bam*HI sites at the 5′ and 3′ ends of the gene, respectively, and were used to subclone the fragment into the pET-3a vector (Novagen Inc.). DNA encoding *R. rhodochrous* dehalogenase (*Rr*DHL) was amplified using the polymerase chain reaction and cloned into the pET-3a vector. For sequencing, the subcloned fragment in pET-3a was transformed into competent *E. coli* DH5α (Novagen, Inc.). W175F and W175Y *Xa*DHL mutations were created using PCR-based point mutagenesis (*21*). The mutated dehalogenase genes were recloned into the pET-3a vector. For overexpression of wild-type and mutant dehalogenases, the pET-3a vector was transformed into competent *E. coli* BL21(DE3). Clones were confirmed by DNA sequencing using the dideoxy-terminator cycle-sequencing method using an Applied Biosystems 373 sequencer (Foster City, CA) (*22*).

Cell Culture and Induction. Freezer stocks of *E. coli* BL21-(DE3) pET-3a (maintained in 10% glycerol, −80 °C) were used to inoculate Luria−Bertani agar plates supplemented with ampicillin (50 μg/mL) (*23*). Single colonies were selected and used to inoculate two 10 mL cultures of Luria−Bertani medium containing 50 μg/mL ampicillin. The cells were cultured for 8 h at 37 °C with shaking (220 rpm), after which time 2 mL of these cultures was used to inoculate each of two 50 mL Luria−Bertani solutions containing 50 μg/mL ampicillin, which were grown overnight at 37 °C with shaking. Ten milliliters of this culture was used to inoculate each of six 1 L Luria−Bertani solutions with ampicillin. When the A_{600} of the cultures reached 0.6−0.7, isopropyl 1-thio-β-D-galactopyranoside was added to a final concentration of 0.5 mM, and the cultures were maintained for an additional 4 h at 30 °C with shaking. The cells were then harvested by centrifugation and washed with 10 mM Tris−SO_4, 1 mM EDTA, pH 7.5. The cell pellets were stored at −70 °C prior to cell lysis.

Dehalogenase Purification. Cells were thawed and suspended in 40 mL of 10 mM Tris−SO_4, 1 mM EDTA, pH 7.5. Cells were disrupted by sonication using a Sonifier Cell Disrupter CP50 equipped with a microtip (Ultrasonics Homogenizer). The cell suspension was placed in an ice bath and sonicated at a power setting of 6 for a total of 20 min using a 30 s on/60 s off cycle. The suspension was centrifuged at 19800*g* for 20 min. The cell-free extract was passed through a DEAE-cellulose (Whatman DE−52) column (2.2 cm diameter × 31 cm) that had been equilibrated with 10 mM Tris−SO_4, 1 mM EDTA, pH 7.5. After washing the column, protein was eluted using a 250 mL gradient: 0−300 mM $(NH_4)_2SO_4$ in 10 mM Tris−SO_4, 1 mM EDTA, pH 7.5. Active fractions were pooled and concentrated by ultrafiltration. The concentrated protein was applied to a Bio-Gel P-60 (BioRad) size exclusion column (1.6 cm diameter × 200 cm) and eluted with 10 mM Tris−SO_4, 1 mM EDTA, and 50 mM Na_2SO_4. Protein homogeneity was established by SDS−PAGE.

Steady-State Kinetics. Enzyme activity was assayed using a pH-indicator dye system similar to that used for carbonic anhydrase (*24*, *25*). For steady-state kinetic analysis, buffers were removed from enzyme solutions by dialysis against 50 mM Na_2SO_4 with 1 mM EDTA, pH 8.2. For assays at the pH optimum, 2 mM *m*-nitrophenol (pK_a 8.2, λ_{max} 400 nm) or 40 μM *m*-cresol purple (pK_a 8.3, λ_{max} 578 nm) were used as pH indicators. Taps (pK_a 8.4) was added to a concentration of 1 mM to *m*-cresol purple. The pH dependence of kinetic parameters was determined using a series of pH indicator/buffer pairs as follows (*25*): pH 6.50 and 6.80, chlorophenol red (574 nm)/1 mM Mes; pH 7.20, *p*-nitrophenol (400 nm)/1 mM Mops; pH 7.50 and 7.80, phenol red (557 nm)/1 mM Hepes; pH 8.20 and 8.50, *m*-cresol purple (578 nm)/1 mM Taps; and pH 8.90, thymol blue (590 nm)/1 mM Ches. The dyes were added at a concentration (15−40 μM) to yield an approximately 1 absorbance unit solution. The buffer concentration was 1 mM, and the ionic strength was held constant at 0.1 M with Na_2SO_4. Prior to each kinetic determination, the pH-indicator dye was titrated with a standardized solution of HCl to provide an apparent extinction coefficient. The steady-state kinetic constants for *Xa*DHL were determined at 25 °C. Kinetic constants were calculated from initial rates using the computer program HYPER (*26*). Titration data were fit to an equation of the form $1/K_{ii}$ or $k_{cat} = [a + b(10^{(pH-pK)})]/[1 + 10^{(pH-pK)}]$ using DeltaGraph

Table 1: Steady-State Kinetic Constants of *Xa*DHL and *Rr*DHL[a]

	*Xa*DHL			*Rr*DHL		
substrate	K_m (mM)	k_{cat} (s^{-1})	k_{cat}/K_m (M^{-1} s^{-1})	K_m (mM)	k_{cat} (s^{-1})	k_{cat}/K_m (M^{-1} s^{-1})
1-chloropropane	0.57	0.29	5.1×10^2	0.40	1.6	4.0×10^3
1-bromopropane	0.041	0.61	1.5×10^4	0.24	1.2	5.0×10^3
1-chlorobutane	4.1	0.15	3.7×10^1	0.40	0.86	2.1×10^3
1-bromobutane	0.43	0.44	1.0×10^3	0.35	0.98	2.8×10^3
1,2-dichloroethane	0.37	2.2	5.9×10^3	$\gg 60$[b]		
1,2-dibromoethane	0.01	2.2	2.2×10^5	1.2	6.2	5.2×10^3
1,4-dichlorobutane	$\gg 60$[b]			0.42	1.5	3.6×10^3
1,2-dibromobutane	ND[c]	ND	ND	2.2	1.3	5.9×10^2
1,2-dichloropropane	$\gg 60$[b]			$\gg 60$[b]		
1,2-dibromopropane	0.23	0.60	2.6×10^3	0.84	1.1	1.3×10^3
2-bromo-1-chloropropane	$\gg 34$[b]			2.3	0.63	2.7×10^2
2-chlorobutane	$\gg 60$[b]			9.4	0.32	3.4×10^1
2-bromobutane	$\gg 30$[b]			0.84	0.39	4.6×10^2
cyclopropyl bromide	$\gg 90$[b]			7.2	0.2	2.8×10^1
cyclobutyl chloride	$\gg 80$[b]			2.9	1.1	3.8×10^2
cyclobutyl bromide	$\gg 20$[b]			0.63	1.1	1.7×10^3
methylbromocyclobutane	ND	ND	ND	1.8	0.52	2.9×10^2
cyclopentyl chloride	$\gg 30$[b]			2.8	0.22	7.9×10^1
cyclopentyl bromide	$\gg 20$[b]			≤ 0.05	0.22	4.4×10^3
allyl chloride	4.2	1.6	3.8×10^2	ND[c]	ND	ND
1,3-dibromopropane	0.019	0.68	3.6×10^4	ND[c]	ND	ND
2-chloroethanol	$\gg 148$[b]			$\gg 148$[b]		
2-bromoethanol	1.0	0.65	6.5×10^2	4.2	1.5	3.6×10^2
1,3-dibromo-2-propanol	2.2	1.43	6.5×10^2	0.17	0.35	2.1×10^3
1,3-dichloro-2-propanol	$\gg 36$[b]			$\gg 32$[b]		

[a] Kinetic constants were determined as described under Materials and Methods. The K_m values had errors $\leq 20\%$. The k_{cat} values had errors $\leq 8\%$. [b] Highest substrate concentration checked; rate of proton release was $\ll 0.02$ min^{-1}. [c] ND = not determined. [d] Nonlinear kinetics.

(DeltaPoint, Monterey, CA). The concentration of purified *Xa*DHL (M_r 35 000) solutions was determined from their absorbance at 280 nm ($\epsilon_{280} = 4.87 \times 10^4$ M^{-1} cm^{-1}); *Rr*DHL (M_r 33 000) concentrations were determined using the Bradford assay (*27*).

Product Inhibition Studies. Chloride, bromide, iodide, and 2-chloroethanol were tested as product inhibitors under initial velocity conditions. *Xa*DHL inhibition was studied with varied concentrations of product against varied concentrations of 1,2-dichloroethane (0.42−2.2 mM) at pH 8.2 and 25 °C. For *Rr*DHL, the varied substrate was 1-chlorobutane (0.22−1.6 mM). The initial velocities were determined in duplicate, using the pH-indicator dye assay described above. Data were fit to equations for competitive, noncompetitive, and uncompetitive inhibition using the computer programs COMP, NONCOMP, and UNCOMP (*26*). The best fit was evaluated by comparison of the standard errors and variance.

RESULTS AND DISCUSSION

pH-Indicator Assay. We developed an assay based on the pH-indicators *m*-nitrophenol and *m*-cresol purple. Because they were to be used as buffers in the assay mixture, pH-indicator dyes were selected so that their pK_a matched the pH optimum of the enzyme (8.2). Prior to the assay, Tris buffers were removed from the enzyme solutions by dialysis. The relatively low extinction coefficient ($\epsilon_{400} = 1200$) of *m*-nitrophenol allowed it to be used directly as the buffer in the assay mixture. *m*-Cresol purple (p$K_a = 8.3$) ($\epsilon_{578} \approx 40\,000$) was mixed with Taps buffer (pH 8.3) to yield a buffer with an effective extinction coefficient of ≈1000. Because products of the dehalogenase are the elements of a strong acid (H^+Cl^-), the rate of production of hydrogen ions could be calculated directly from the rate change in absorbance. Reactions initiated with the addition of the enzyme showed linear changes in absorbance from zero time. Rates were determined from total changes of <0.1 absorbance, which for the *m*-nitrophenol system represented a change in pH of <0.06. The steady-state kinetic constants for *Xa*DHL were determined either in the presence of 2 mM *m*-nitrophenol (pH 8.2) or in the combination of 40 μM *m*-cresol purple and 1 mM Taps (pH 8.2). Identical K_m and k_{cat} values were obtained using both dye systems. *m*-Nitrophenol caused a 10-fold increase in K_m values for the *Rr*DHL enzyme; therefore, the steady-state constants for *Rr*DHL were determined using *m*-cresol purple and Taps.

This assay was used to determine the steady-state kinetic constants for *Xa*DHL using a variety of halogenated substrates (Table 1). As discussed in more detail below, the results presented here for *Xa*DHL are qualitatively similar to those reported by Janssen and co-workers, who used conventional halide release assays to determine steady-state kinetic parameters. Our experiments, carried out at 25 °C, had slightly lower rates than those reported by Janssen and co-workers, who carried out assays at 30 or 37 °C. Using this pH-indicator assay, we have identified new substrates for *Xa*DHL, examined product inhibition of this enzyme, and characterized the *Rhodococcus* enzyme.

Substrate Specificity of XaDHL and RrDHL. The Michaelis constant (K_m), k_{cat}, and catalytic efficiency (k_{cat}/K_m) of *Xa*DHL and *Rr*DHL were determined for a number of haloalkanes (Table 1). All of these substrates showed normal Michaelis−Menten behavior over the range of concentrations investigated with *Xa*DHL. The substrate specificity trends reported in Table 1 are in general agreement with those reported by Janssen and co-workers (*11*, *12*). The *Xa*DHL uses only primary alkyl halides as substrates, and k_{cat}/K_m values of *Xa*DHL decrease as the chain length of the primary haloalkane increases. 1,2-Dichloroethane and 1,2-dibromo-

ethane have the highest k_{cat} and k_{cat}/K_m values. Consistent with previous results, K_m values for the brominated substrates are at least 10-fold lower than the corresponding chlorinated substrates. The lower K_m for brominated substrates reflects not only a tighter affinity of the enzyme ($K_s = k_{-1}/k_1$) for brominated compounds but also a faster rate for bromide displacement (k_2, Scheme 1) (*11*, *12*).

The substrate specificity of the *Rr*DHL enzyme was examined using the *m*-cresol purple/Taps-based pH-indicator assay. With the exception of 2-bromo-1-chloropropane, all substrates displayed normal Michaelis−Menten behavior over the range of concentrations investigated. Although not as pronounced as for the *Xa*DHL, the *Rr*DHL has a modest K_m preference for brominated versus chlorinated substrates. The *Rhodococcus* enzyme has a much broader specificity for the hydrolysis of alkyl halides than the *Xanthobacter* enzyme. For example, *Rr*DHL uses 1-halopropanes and 1-halobutanes with equal catalytic efficiency. In addition, secondary alkyl halides are substrates for *Rr*DHL.

The differential activities against the secondary alkyl halides suggest differences in the mechanisms of *Xa*DHL and *Rr*DHL. *Xa*DHL is thought to proceed via an S_N2 type mechanism primarily because of its absolute specificity for primary alkyl halides. In contrast with this requirement, the *Rr*DHL utilizes secondary as well as primary alkyl halides as substrates (Table 1). While 2-chloropropane and 2-bromopropane are not substrates for either enzyme, *Rr*DHL dehalogenates 2-chlorobutane and 2-bromobutane. In addition to dehalogenating linear secondary alkyl halides, the *Rhodococcus* enzyme will turn over the hindered cyclic alkyl halides. Within this series of substrates, *Rr*DHL has the highest efficiencies toward cyclobutyl chloride, cyclobutyl bromide, and cyclopentyl bromide.

Based on both k_{cat} and k_{cat}/K_m, 1,2-dibromoethane is the best substrate for both dehalogenases. Interestingly, 1,2-dichloroethane is not a substrate for *Rr*DHL ($K_m \gg 60$ mM) while it is among the best substrates for the *Xanthobacte*r enzyme. Even at concentrations up to 60 mM, we cannot detect turnover of 1,2-dichloropropane by either *Xa*DHL or *Rr*DHL. However, both enzymes have similar k_{cat}/K_m values for 1,2-dibromopropane. The *Xanthobacter* enzyme is not active toward 2-bromo-1-chloropropane, while *Rr*DHL has substantial activity for hydrolysis of this substrate. Taken together these data suggest that the *Rr*DHL, capable of secondary alkyl halide hydrolysis, displaces bromide from 2-bromo-1-chloropropane. *Xa*DHL, only capable of primary alkyl halide hydrolysis, does not use 2-bromo-1-chloropropane as a substrate. *Rr*DHL has similar efficiency for 1,2-dibromobutane as it does for 1,2-dibromopropane.

While halohydrins are the products of enzymatic dehalogenation of 1,2-dihaloalkanes, they are also potential substrates. Using our assay, neither enzyme is active against 2-chloroethanol ($K_m \gg 148$ mM) or 1,3-dichloro-2-propanol ($K_m \gg 36$ mM). *Xa*DHL and *Rr*DHL are both active on 2-bromoethanol and 1,3-dibromo-2-propanol, with *Rr*DHL showing a higher catalytic efficiency for the latter substrate.

The *Rr*DHL prefers larger molecules as substrates as evidenced by its ability to dehalogenate longer linear chain and cyclic hydrocarbons when compared with the *Xa*DHL. The k_{cat} values for 1-chloro- and 1-bromobutane are similar, suggesting that, as with *Xa*DHL, displacing the halide is not rate-limiting. The K_m values for brominated substrates may be overestimated because of their instability in solution; however, the K_m trends reported in this table are clear. All of the differences in substrate specificities between the two enzymes provide strong evidence for mechanistic differences in these dehalogenases.

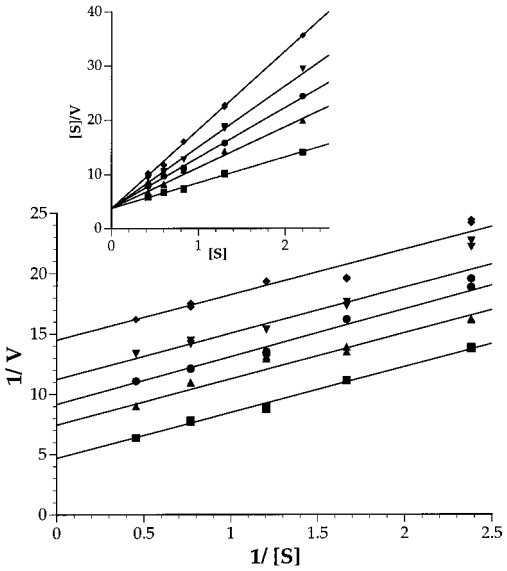

FIGURE 3: Lineweaver−Burk ($1/V$ vs $1/S$) and Hanes−Woolf (inset, V/S vs S) plots demonstrating uncompetitive inhibition of *Xa*DHL by chloride. The rate of dehalogenation of 1,2-dichloroethane was determined using the pH-indicator assay. Rates were obtained in duplicate in the presence of 0 mM Cl^- (■), 10 mM Cl^- (▲), 18 mM Cl^- (●), 27 mM Cl^- (▼), and 40 mM Cl^- (◆). Lines were fit to the data using the program Enzyme Kinetics (Trinity Software, Compton, NH).

Product Inhibition Patterns. We examined the product inhibition patterns for both *Xa*DHL and *Rr*DHL. The product of 1,2-dichloroethane hydrolysis, 2-chloroethanol, did not inhibit *Xa*DHL when 1,2-dichloroethane was the varied substrate. Inhibition of *Xa*DHL 1,2-dichloroethane hydrolysis by chloride was analyzed using a Lineweaver−Burk plot (Figure 3). The parallel lines are consistent with uncompetitive inhibition. Further evidence was obtained by replotting the data using the Hanes−Woolf equation (Figure 3 inset), and a common intercept was observed, indicating that the slopes from the Lineweaver−Burk plot are constant (*28*). More convincingly, the data were analyzed by fitting the equations for uncompetitive, competitive, and noncompetitive inhibition using the computer programs UNCOMP, NONCOMP, and COMP (*26*). The best fit was evaluated by comparison of the standard errors and variance. The only consistent fit was to that of uncompetitive inhibition with a $K_{ii} = 19 \pm 0.91$ mM for chloride. Bromide ($K_{ii} = 2.5 \pm 0.19$ mM) and iodide ($K_{ii} = 4.1 \pm 0.43$ mM) are also uncompetitive inhibitors of *Xa*DHL. At similar concentrations, NaF does not inhibit *Xa*DHL. 1,2-Dibromoethane was also employed as the varied substrate to test halide inhibition. We observed no change in the inhibition constants or patterns. Clearly, halides are uncompetitive and not competitive inhibitors of *Xa*DHL.

We examined the effect of pH on chloride inhibition of *Xa*DHL. Using 1,2-dichloroethane as the varied substrate, we determined the K_{ii} for chloride at nine pHs between 6.5 and 8.9. The chloride inhibition pattern was uncompetitive at all pH values, and the affinity of *Xa*DHL for chloride

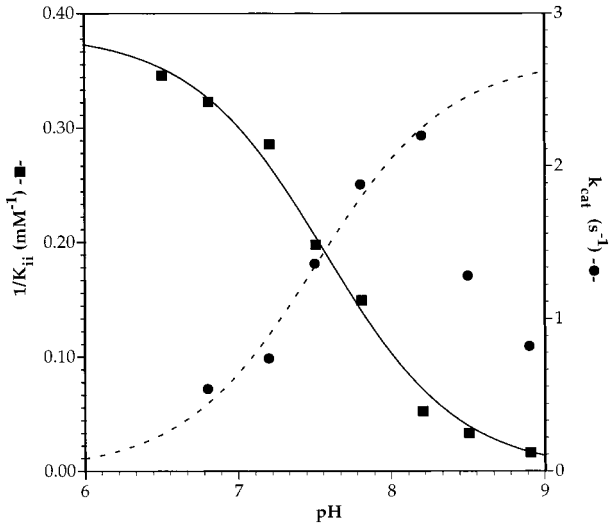

FIGURE 4: pH dependence of K_{ii} (■) for chloride and k_{cat} (●) of *Xa*DHL. The inhibition constants were determined using 1,2-dichloroethane as the varied substrate (0.42−2.0 mM). The dissociation constants for chloride at each pH were determined by fitting the data to the equation for uncompetitive inhibition (*26*). The standard error values for the K_{ii} and k_{cat} were ≤15% and ≤8%, respectively. The solid line is a least-squares fit of $1/K_{ii}$ to a single ionization with a pK_a of 7.56 ($r^2 = 0.993$). At low pH, the limit of K_{ii} is 2.6 mM while at high pH the limit of $1/K_{ii}$ is 0. The dashed line is a least-squares fit of k_{cat} to a single pK_a of 7.55 ($r^2 = 0.979$) and a maximum $k_{cat} = 2.74$ s^{-1} and a minimum $k_{cat} = 0.062$ s^{-1}.

increased at lower pH. The K_{ii} for chloride decreased more than 20-fold from 61 mM at pH 8.9 to 2.9 mM at pH 6.5. A plot of $1/K_{ii}$ versus pH (Figure 4) showed simple proton titration behavior that was fit by a single pK_a of 7.56. Evident from both the titration data and the least-squares fit (Figure 4), $1/K_{ii}$ approaches zero at pH >9. Apparently chloride does not bind to *Xa*DHL when a proton is dissociated from an ionizable group on the enzyme with a pK_a of approximately 7.5. The k_{cat} for 1,2-dichloroethane shows more complex titration behavior in this pH range. The k_{cat} increased with pH to a maximum at pH 8.2 and then decreased rapidly at more alkaline pH (Figure 4). The pH dependence of k_{cat} on the acid side of the pH optimum followed simple titration behavior and was also fit to a single pK_a of 7.55. Association of a proton with an ionizable group (pK_a = 7.55) on *Xa*DHL renders the enzyme inactive. Apparently the rate of *Xa*DHL and its affinity for chloride are both affected by an ionizable group with a pK_a of approximately 7.5. Of the ionizable groups present in proteins, a pK_a of 7.5 is most consistent with the imidazole side chain of a histidyl residue. Of the five histidines in *Xa*DHL, the most likely to yield the titration behavior of both k_{cat} and K_{ii} for halides is the active site H289 (Figure 1).

Halides were tested as inhibitors of *Rr*DHL using 1-chlorobutane as the varied substrate. In contrast to *Xa*DHL, the halides did not inhibit *Rr*DHL even at 80 mM halide. There was no inhibition even after lowering the pH from 8.2 to 7.2.

Product inhibition studies can aid in determining a kinetic mechanism. We observed uncompetitive inhibition of *Xa*DHL by the halides. As uncompetitive inhibitors, halides do not bind to the free form of the enzyme and cannot be the last product released from the enzyme (*26*). The pH dependence of the chloride inhibition constants indicates that the halides bind to a protonated form of the enzyme. Because we do not observe inhibition by 2-chloroethanol, the steady-state kinetic data do not allow further speculation on the order of release of the products (alcohol, halide, or hydrogen ion) from the enzyme.

Table 2: Steady-State Kinetic Constants for W175F and W175Y *Xa*DHL[a]

	1,2-dichloroethane			1,2-dibromoethane		
enzyme	K_m (mM)	k_{cat} (s^{-1})	k_{cat}/K_m (M^{-1} s^{-1})	K_m (mM)	k_{cat} (s^{-1})	k_{cat}/K_m (M^{-1} s^{-1})
wild type	0.37	2.2	5.9×10^3	0.01	2.2	2.2×10^5
W175F	3.0	0.42	1.4×10^2	0.05	0.79	1.6×10^4
W175Y	2.7	0.20	7.4×10^1	0.05	1.6	3.2×10^4

[a] Kinetic constants were determined as described under Materials and Methods. The K_m values had errors ≤20%. The k_{cat} values had errors ≤8%.

Characterization of W175F and W175Y XaDHL. *Rr*DHL does not have a tryptophan residue corresponding to that at position 175 in *Xa*DHL, and it is not inhibited by halides. Because W175 has been implicated in halide binding in *Xa*DHL (*8*), we used site-directed mutagenesis to examine its role in halide inhibition. W175 was mutated to a phenylalanine or a tyrosine residue, and the effect of these mutations on enzyme activity was determined using 1,2-dibromoethane and 1,2-dichloroethane as substrates (Table 2). Significantly, substitution of the W175 with phenylalanine or tyrosine did not have a dramatic effect on either the rate of hydrolysis (<3-fold) or the K_m (5-fold) for 1,2-dibromoethane. Given these modest changes of K_m and k_{cat} in W175F and W175Y, tryptophan 175 does not appear to be critical for turnover of 1,2-dibromoethane by *Xa*DHL. These results are qualitatively consistent with experimental results reported by Janssen and co-workers (*29*) as well as the theoretical results reported by Lightstone and Bruice (*14*−*16*). The molecular dynamics simulations showed that only W125 is involved in chlorine binding in the ES complex. In the S_N2 transition state, the simulations predict the equidistant hydrogen bonds from both W125 and W175 contribute to the stabilization of the leaving chlorine. However, the hydrogen bond stabilization of the chloride is expected to contribute only modestly (1−2 kcal/mol) to lowering of the activation energy (*15*). The k_{cat} for the hydrolysis of 1,2-dichloroethane by W175F was decreased 5-fold compared to wild-type *Xa*DHL, while the K_m increased 10-fold. This implies that W175 is more involved in the activation of the C−Cl bond. As postulated by Janssen and co-workers, the increase in K_m results from changes in the affinity for the substrate (K_s) as well as the decreased rate of halide displacement (k_2, Scheme 1). A similar result is observed for *Xa*DHL when W125 was mutated to a phenylalanine residue; however, the W125F mutant had an increased K_m for both 1,2-dichloroethane and 1,2-dibromoethane (*17*).

Next, we examined halides as product inhibitors of W175F and W175Y mutants of *Xa*DHL. Halides (Cl^-, Br^-, or I^- up to 80 mM) do not inhibit W175F at either pH 7.2 or pH 8.2. Likewise, W175Y is not inhibited by halides under similar conditions. The fact that halides do not inhibit the mutants suggests that tryptophan 175 is involved in halide ion binding. Crystallographic studies and molecular dynamics simulations predict that both W125 and W175 play a role in halide binding to *Xa*DHL (*15*, *30*). Consistent with our

observation that W175 is required for halide binding to *Xa*DHL, halides do not inhibit *Rr*DHL, which has no analogous tryptophan residue.

CONCLUSIONS

We have developed and used a pH-indicator dye-based proton release assay to probe the specificity of *Rr*DHL and *Xa*DHL. Both enzymes catalyze the hydrolysis of short-chain primary alkyl halides. However, the specificity of *Rr*DHL is much broader, encompassing linear, secondary, and cyclic alkyl halides. *Rr*DHL was not inhibited by halides at concentrations up to 80 mM. The lack of halide inhibition and broader substrate range suggests that the mechanism by which *Rr*DHL dehalogenates is different in detail from that of *Xa*DHL.

Significantly, bromide, chloride, and iodide inhibit *Xa*-*DHL*. Moreover, halides are uncompetitive inhibitors of *Xa*DHL with respect to 1,2-dihaloethanes; therefore, halide cannot bind to the free form of the enzyme and cannot be the last product released. At very high pH, chloride does not bind to the enzyme. The affinity of *Xa*DHL for chloride increases significantly at lower pH, suggesting that halide binds to a protonated form of the enzyme. Simple titration behavior of both k_{cat} and the chloride inhibition constant indicates that the critical ionizable group on *Xa*DHL has a pK_a of approximately 7.5, consistent with the side chain of histidine. Our view is that chloride binding to *Xa*DHL requires protonation of the side chain of the active site H289 to imidazolium. Consistent with this view, the crystal structure of *Xa*DHL (*8*) obtained in the presence of chloride and under acidic conditions (pH 5.2) would be that of the inhibited complex of *Xa*DHL·H^+·Cl^-. In this structure, both D260 (3.31 Å, N_δ) and D124 (2.34 Å, N_ϵ) are within hydrogen bonding distance of the side chain of H289, which is compatible with it being present as imidazolium. The bound halide is located at equal distance from the N_η of W125 (3.4 Å) and N_η of W175 (3.3 Å). In agreement with this structure, our mutagenesis studies indicate that, though not necessary for activity, W175 is required for halide binding.

The kinetic mechanism as proposed by Janssen and co-workers (*11, 12, 29, 31, 32*) does not account for one product, namely, the hydrogen ion. In addition, they propose that chloride is the last product released from the enzyme. Their pre-steady-state kinetic studies have clearly shown that the alcohol is the first product released from the enzyme (*12*). Combined with the results presented here, we believe that the order of product release from *Xa*DHL dehalogenation is alcohol, followed by chloride, followed by a hydrogen ion.

ACKNOWLEDGMENT

We thank Dr. Barry M. Willardson (Department of Chemistry and Biochemistry, Brigham Young University) for providing clones containing wild-type dehalogenase.

REFERENCES

1. Janssen, D. B., Scheper, A., Dijkhuizen, L., and Witholt, B. (1985) *Appl. Environ. Microbiol. 49*, 673−677.
2. Kulakova, A. N., Stafford, T. M., Larkin, M. J., and Kulakov, L. A. (1995) *Plasmid 33*, 208−217.
3. Curragh, H., Flynn, O., Larkin, M. J., Stafford, T. M., Hamilton, J. T. G., and Harper, D. B. (1994) *Microbiology* (Reading, U.K.) *UK 140*, 1433−1442.
4. Dolfing, J., van den Wijngaard, A. J., and Janssen, D. B. (1994) *Biodegradation 4*, 261−282.
5. Janssen, D. B., and Witholt, B. (1985) *Sci. Total Environ. 47*, 121−135.
6. Stucki, G., and Thuer, M. (1994) *Appl. Microbiol. Biotechnol. 42*, 167−172.
7. Verschueren, K. H., Franken, S. M., Rozeboom, H. J., Kalk, K. H., and Dijkstra, B. W. (1993) *J. Mol. Biol. 232*, 856−872.
8. Verschueren, K. H. G., Seljee, F., Rozeboom, H. J., Kalk, K. H., and Dijkstra, B. W. (1993) *Nature 363*, 693−698.
9. Pries, F., Kingma, J., Krooshof, G. H., Jeronimus-Stratingh, C. M., Bruins, A. P., and Janssen, D. B. (1995) *J. Biol. Chem. 270*, 10405−10411.
10. Pries, F., Kingma, J., Pentenga, M., van Pouderoyen, G., Jeronimus-Stratingh, C. M., Bruins, A. P., and Janssen, D. B. (1994) *Biochemistry 33*, 1242−1247.
11. Schanstra, J. P., and Janssen, D. B. (1996) *Biochemistry 35*, 5624−5632.
12. Schanstra, J. P., Kingma, J., and Janssen, D. B. (1996) *J. Biol. Chem. 271*, 14747−14753.
13. Damborsky, J., Kuty, M., Nemec, M., and Koca, J. (1997) *J. Chem. Inf. Comput. Sci. 37*, 562−568.
14. Lightstone, F. C., Zheng, Y.-J., Maulitz, A. H., and Bruice, T. C. (1997) *Proc. Natl. Acad. Sci. U.S.A. 94*, 8417−8420.
15. Lightstone, F. C., Zheng, Y.-J., and Bruice, T. C. (1998) *J. Am. Chem. Soc. 120*, 5611−5621.
16. Lightstone, F. C., Zheng, Y.-J., and Bruice, T. C. (1998) *Bioorg. Chem. 26*, 169−174.
17. Kennes, C., Pries, F., Krooshof, G. H., Bokma, E., Kingma, J., and Janssen, D. B. (1995) *Eur. J. Biochem. 228*, 403−407.
18. Janssen, D. B., Pries, F., van der Ploeg, J., Kazemier, B., Terpstra, P., and Witholt, B. (1989) *J. Bacteriol. 171*, 6791−6799.
19. Bergman, J. G., and Sanik, J. (1957) *Anal. Chem. 29*, 241−243.
20. Saiki, R. K., Gelfand, D. H., Stoffel, S., Scharf, S. J., Higuchi, R., Horn, G. T., Mullis, K. B., and Erlich, H. A. (1988) *Science 239*, 487−491.
21. Zhao, L. J., Zhang, Q. X., and Padmanabhan, R. (1993) *Methods Enzymol. 217*, 218−227.
22. Sanger, F., Nicklen, S., and Coulsen, A. R. (1977) *Proc. Natl. Acad. Sci. U.S.A. 74*, 5463−5467.
23. Sambrook, J., Fritsch, E. F., and Maniatis, T. (1989) in *Molecular Cloning: A Laboratory Manual* (Nolan, C., Ed.) 2nd ed., p A1, Cold Spring Harbor Laboratory Press, Cold Spring Harbor, NY.
24. Hurt, J. D., Tu, C., Laipis, P. J., and Silverman, D. N. (1997) *J. Biol. Chem. 272*, 13512−13518.
25. Khalifah, R. (1971) *J. Biol. Chem. 246*, 2561−2573.
26. Cleland, W. W. (1979) *Methods Enzymol. 63*, 103−138.
27. Bradford, M. M. (1976) *Anal. Biochem. 72*, 241−254.
28. Cooper, B. F., and Rudolph, F. B. (1995) *Methods Enzymol. 249*, 188−211.
29. Krooshof, G. H., Ridder, I. S., Tepper, A. W. J. W., Vos, G. J., Rozeboom, H. J., Kalk, K. H., Dijkstra, B. W., and Janssen, D. B. (1998) *Biochemistry 37*, 15013−15023.
30. Verschueren, K. H. G., Kingma, J., Rozeboom, H. J., Kalk, K. H., Janssen, D. B., and Dijkstra, B. W. (1993) *Biochemistry 32*, 9031−9037.
31. Schanstra, J. P., Ridder, I. S., Heimeriks, G. J., Rink, R., Poelarends, G. J., Kalk, K. H., Dijkstra, B. W., and Janssen, D. B. (1996) *Biochemistry 35*, 13186−13195.
32. Krooshof, G. H., Kwant, E. M., Damborsky, J., Koca, J., and Janssen, D. B. (1997) *Biochemistry 36*, 9571−9580.

BI982853Y